

Magnetism in Ni-based binary alloys

T. Hoshino and M. Asato

Department of Applied Physics, Faculty of Engineering, Shizuoka University, Hamamatsu 432-8561, Japan
Fax:81-53-478-1276, e-mail:tsthosh@eng.shizuoka.ac.jp

The magnetism in Ni-based binary alloys (NiX, X=Ti, V, Cr, Mn, Fe, Co, Cu) is examined by use of the first-principles calculations for impurity-impurity interaction energies of X-X in Ni. The calculations are based on the density-functional theory in the local-spin-density approximation and the Korringa-Kohn-Rhostoker Green's function method is applied for impurities. We show that the observed ordering-behavior of NiX (X=Mn, Fe, Co) can never be explained without the magnetic effect. The importance of magnetism in Ni-based alloys is discussed by comparing with the calculated results for non-magnetic Pd-based alloys (PdX, X=Zr, Nb, Mo, Tc, Ru, Rh, Ag), being isoelectronic to magnetic Ni-based alloys.

Key words: Magnetism in Ni-based alloys, impurity-impurity interaction, density-functional theory, KKR-Green's function method

1. INTRODUCTION

We have shown that the fundamental features about segregation, miscibility, and order of binary alloys may be explained by use of the impurity-impurity interaction energies in metals; the minor constituent of the binary alloy may be considered as an impurity element, while the major constituent becomes a host element. As discussed in Refs.1 and 2, the interaction energy E_{int} between two X impurities in the host H is defined as the total-energy difference between two states (atomic configurations), shown in Figs.1; (a) the initial one where both X impurities are infinitely apart and (b) the final state where the two X impurities are located at nearest-neighbor sites.^{1,2}

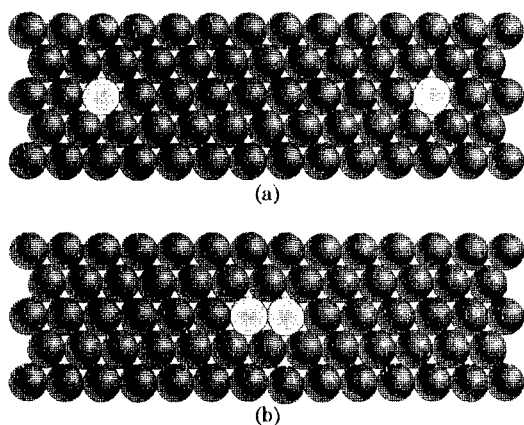


Fig.1 The nearest-neighbor impurity-impurity interaction energy is defined as the total-energy difference between two states; (a) initial state and (b) final state, where the impurity (X) and host (H) elements are shown by \circ and \bullet .

As a result of this definition, it is easily understood that negative energies of E_{int} correspond to attractive interaction between the impurity atoms, while positive ones to repulsive interaction. We have already shown that the fundamental features for phase diagrams may be explained (or predicted) by use of the calculated results. For example, the observed phase diagrams of Pd-based alloys (Figs.2)³ are explained by the calculated results (X-X in Pd, X=Zr~Ag), being also shown in Fig.3 and Table 1,⁴ as follows;

(1) The observed experimental phase diagram of PdZr (Fig.2(a)), being ordering behavior, is explained by the large positive value ($E_{int} \sim 1.5\text{eV}$) because the atoms of the impurity elements become surrounded with the atoms of the host element as a result of the repulsive interaction of the impurity pair.

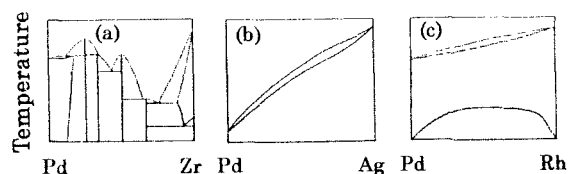


Fig.2 Typical three kinds of phase diagrams for binary alloys are shown; (a) ordering (PdZr), (b) continuous solid solution (PdAg), and (c) segregation below 800~1000K ($0.06 \sim 0.08\text{eV}$) and disorder above 800~1000K (PdRh). The differences among (a), (b), and (c) are predicted by use of the sign and magnitude of E_{int} (impurity-impurity interaction energy in Pd; impurity=Zr, Ag, Rh); (a), (b), and (c) correspond to $E_{int} \sim 1.5\text{eV}$, $E_{int} \simeq 0$, and $E_{int} \sim -0.06\text{eV}$, respectively. See a text for details.

(2) The observed experimental phase diagram of PdAg (Fig.2(b)), being continuous solid solution, is explained by the very small value ($E_{int} \sim 0.0\text{eV}$) because the small value means the small difference between the impurity and host elements.

(3) The observed experimental phase diagram of PdRh (Fig.2(c)), being segregation below $800\sim 1000\text{K}$ ($0.06\sim 0.08\text{ eV}$) and disorder above $800\sim 1000\text{K}$, is explained by the small negative value of $E_{int} \sim -0.06\text{ eV}$. At low temperatures the impurity atoms form clusters to gain the internal energy, while at high temperatures the Rh impurity atoms become soluble in Pd, due to the entropy term in the free energy.

The purpose of the present paper is to elucidate the importance of the magnetism in NiX ($X=\text{Ti}\sim\text{Cu}$) alloy by use of the first principle calculations for interaction energies between two identical X impurities in Ni. The experimentally known ordering behavior of NiFe and NiCo is very different from the experimentally known segregation behavior of PdRu and PdRh,³ being isoelectronic to NiFe and NiCo. A detailed description of our method is reported in Refs. 1, 2, and 4. Here we only mention that the present calculations use two approximations; (1) spherical potentials are used to solve Kohn-Sham equations and (2) a cutoff $l_{max} = 3$ is used to truncate the angular momentum expansions of the Green's functions and wave functions.

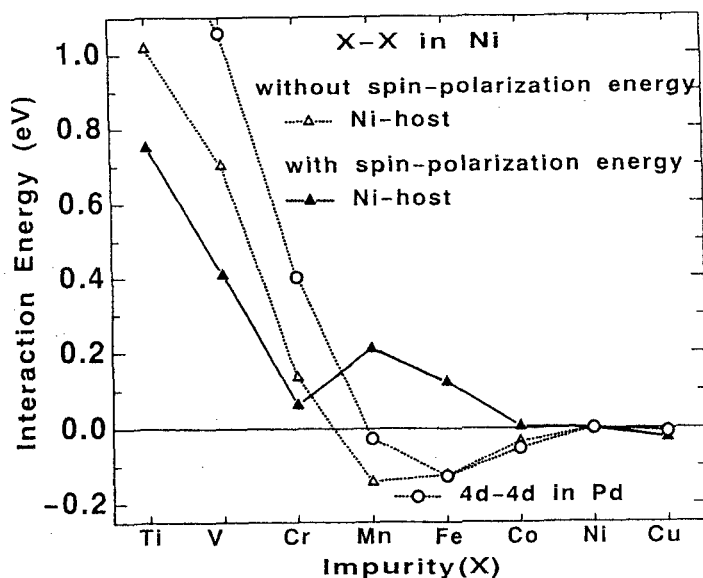


Fig.3 Interaction energies between two identical impurities (Ti~Cu) in Ni. The calculated results without spin-polarization effect (Δ) as well as with spin-polarization effect (\blacktriangle). Interaction energies between two identical impurities ($X=\text{Zr}\sim\text{Ag}$) in Pd, being isoelectronic to X-X ($X=\text{Ti}\sim\text{Cu}$) in Ni, are also shown for a comparison. The value ($E_{int} \sim 1.5\text{eV}$) of Zr-Zr in Pd is out of the figure.

Table I. Calculated nearest-neighbor interaction energies E_{int} of impurity pairs (Ti~Cu) in Ni (in eV). The calculated results without spin-polarization effect as well as with spin-polarization effect are listed to show the importance of magnetism. Negative energies mean attractive, positive ones repulsive interaction. The calculated results for impurity pairs (Zr~Ag) in Pd, being isoelectronic to impurity pairs (Ti~Cu) in Ni, are also shown for a comparison.

impurity	Ti	V	Cr	Mn	Fe	Co	Ni	Cu
Ni-host (with spin-polarization)	0.75	0.41	0.06	0.21	0.12	0.01	-0.03	-0.01
Ni-host (without spin-polarization)	1.02	0.70	0.14	-0.14	-0.12	-0.04	-0.01	-0.01
impurity	Zr	Nb	Mo	Tc	Ru	Rh	Pd	Ag
Pd-host (non-magnetic)	1.48	1.09	0.41	-0.03	-0.13	-0.06	-0.01	-0.01

2. CALCULATED RESULTS

Figure 3 and Table I show the calculated results for X-X ($X=\text{Ti}\sim\text{Cu}$) interaction energies in Ni (magnetic system), together with those for X-X ($X=\text{Zr}\sim\text{Ag}$) in Pd (non-magnetic system), being isoelectronic to X-X in Ni; the value of $E_{int} \sim 1.5\text{eV}$ for Zr-Zr in Pd is very large and is not shown in Fig.3. In order to examine the magnetic effect for X-X in Ni, we carried out the calculations without spin-polarization effect as well as with spin-polarization effect. It is found that the values of E_{int} for 3d-3d in Ni, without spin-polarization effect, agree with those of E_{int} for 4d-4d in Pd. However, it is also found that E_{int} for Mn-Mn and Fe-Fe in Ni, change very much by the inclusion of magnetism; the energy gain occurs for Ti~Cr, while the energy loss for Mn~Co. For Mn~Co the sign of E_{int} also changes from negative (attraction, segregation at low temperatures) to positive (repulsion,

ordering). We found that all the calculated results with spin-polarization effect (large positive values for Ti~Fe and very small values for Co and Cu) seem to agree with the experimental phase diagrams for NiX ($X=\text{Ti}\sim\text{Cu}$): NiTi, NiV, NiCr, NiMn, and NiFe are alloys of ordered compounds, while NiCo and NiCu are of continuous solid solutions. The parabolic behavior around Mn, Fe, and Co, obtained by the calculations without spin-polarization effect, may be understood in terms of the filling of the virtual bound states which are broadened due to the strong covalent interaction between the d states on the nearest-neighboring sites.^{2,5} The strong repulsion around early transition-metal impurities may be understood by considering the repulsive interaction between ionic cores, being large for the early transition-metal impurities with the large Wigner-Seitz radius. The inverse dip around Mn, Fe, and Co, due to magnetism may also be explained by considering the change of magnetic

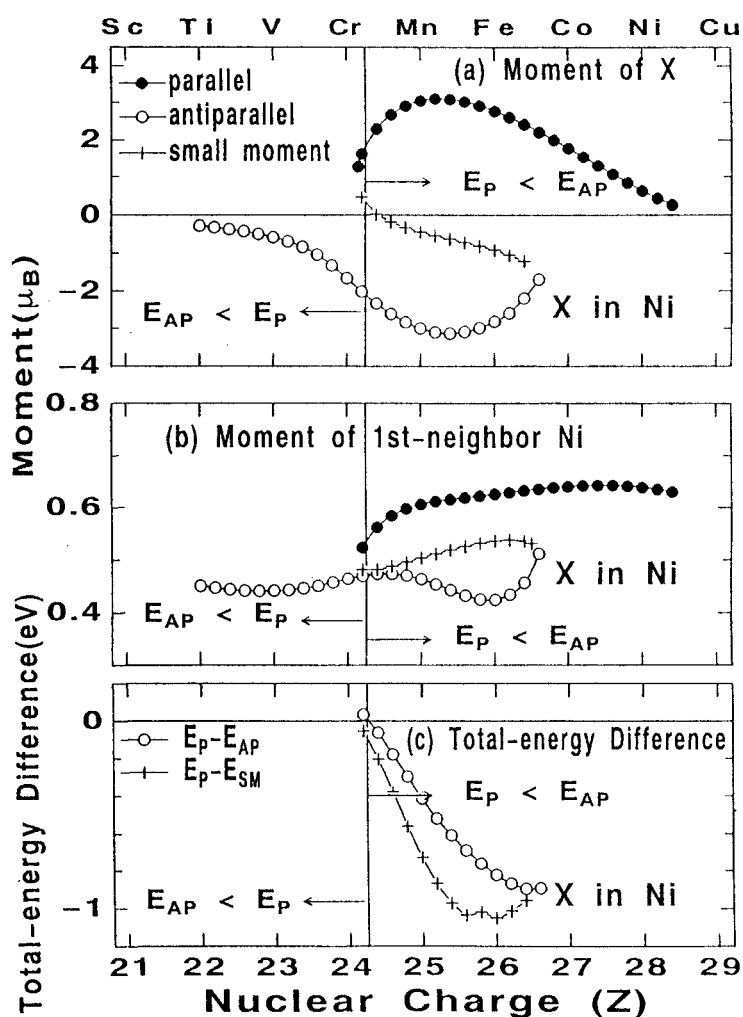


Fig.4 (a) Local magnetic moments (MM's) for 3d impurities in Ni; the three kinds of solutions exist for $24.2 \leq Z \leq 26.7$; two solutions of parallel and antiparallel MM's to the bulk magnetization and a solution of a very small MM. (b) The three kinds of MM's of nearest-neighbor Ni atoms around impurities, each of which correspond to one of three MM solutions of impurities. (c) The total-energy differences between the two solutions of parallel-MM and antiparallel-MM and between the two solutions of parallel-MM and small-MM.

moments (MM's), caused by pairing of impurities.⁵

Here we examine the magnetism in Ni-based alloys. We start with the discussion of single 3d impurities in Ni. For a magnetic 3d impurities in a paramagnetic host such as Cu, it is well known that there are three solutions; one being non-magnetic (unstable) and two doubly degenerate and magnetic (stable, up and down spin configurations with equal magnetic moment). On the other hand, for a magnetic 3d impurity in a ferromagnetic Ni, a non-magnetic solution shifts to a solution of a very small moment and the degeneracy of the magnetic solutions is lifted, as seen in Fig.4(a). Two solutions of parallel and antiparallel magnetic moments (MM's) to the bulk magnetization exist for $24.2 \leq Z \leq 26.7$ (Z is a nuclear charge). From total-energy calculations, it is found that for $Z \geq 24.3$ the MM parallel and for $Z \leq 24.2$ the MM antiparallel to the bulk magnetization is stable. The change of MM's of Ni atoms at nearest-neighbor sites of a 3d impurity is also shown in Fig.4(b), strongly depending on a magnetic state of 3d impurities. It is noted that for a solution of antiparallel MM of a single 3d impurity, the decrease of MM's of nearest-neighbor Ni atoms becomes very large and leads to the large magnetic energy loss. Now we discuss the total-energy change caused by pairing of 3d magnetic impurities. As have already been discussed for 3d impurities in Cu,⁵ the MM's of impurities (Mn, Fe, Co) decrease (0.07 for Mn, 0.06 for Fe, 0.02 for Co) by pairing of impurities. The decrease of MM's leads to the magnetic energy loss,⁵ as seen in Fig.3. It is also noted that for these impurity pairs the ferromagnetic coupling is stable⁶ and the perturbation to the MM's of the nearest-neighbor Ni atoms is very small, as seen in Fig.4(b). On the other hand, for Ti~Cr, the MM's of impurities couple antiferromagnetically with the MM's of the surrounding Ni atoms; it is noted that the coupling between impurities is ferromagnetic.⁶ For the antiferromagnetic couplings between impurities and nearest-neighbor Ni atoms, the reduction of MM's of the nearest-neighbor Ni atoms around impurities is very large as seen in Fig. 4(b) and leads to the large energy loss. However, it is noted that the number of nearest-neighbor Ni atoms decrease by pairing of impurities; the number of nearest-neighbor Ni atoms decrease from 24(=2x12) to 18. Thereby the magnetic energy loss due to the decrease of MM's of nearest-neighbor Ni atoms may decrease by pairing of impurities. As a result, the magnetic interaction becomes attraction (energy gain) around Ti~Cr, as seen in Fig.3.

3. SUMMARY AND CONCLUSION

We have shown that the fundamental features of the observed phase diagrams of NiX ($X=\text{Ti}\sim\text{Cu}$) alloys can be explained by use of the present first-principles impurity-impurity interaction energies of X-X in Ni. The importance of magnetism is shown by use of two kinds of calculations with spin-polarization effect and without spin-polarization effect; the impurity-impurity interaction energies of X-X ($X=\text{Mn, Fe, Co}$) in Ni change from negative (attractive) to positive (repulsive) by taking into account the spin-polarization effect and agree with the observed ordering-behavior of NiMn, NiFe, and NiCo.

References

- (1) T. Hoshino, W. Schweika, R. Zeller, and P. H. Dederichs, *Phys. Rev. B* **47**, 5106-5117(1993).
- (2) T. Hoshino, R. Zeller, P. H. Dederichs, and T. Asada, *Computational Physics as a New Frontier in Condensed Matter Research*, edited by H. Takayama *et al.* (Physical Society of Japan, Tokyo, 1995), 105-113.
- (3) *Binary Alloy Phase Diagrams*, edited by T. B. Massalski *et al.*, 2nd ed. (ASM International, New York, 1990)
- (4) T. Hoshino, M. Asato, and K. Masuda-Jindo, *Proceeding of the third pacific rim international conference on advanced materials and processing (PRICM3)*, edited by M. A. Imam *et al.*, 1245-1250(1998).
- (5) T. Hoshino, R. Zeller, P. H. Dederichs, and M. Weinert, *Europhys. Lett.* **24**, 495-500(1993).
- (6) T. Hoshino, R. Zeller, and P. H. Dederichs, *J. Magn. Magn. Mater.* **140-144**, 113-114(1995).

(Received December 11, 1998; accepted February 28, 1999)